Mechanism and Site Requirements for Activation and Chemical Conversion of Methane on Supported Pt Clusters and Turnover Rate Comparisons among Noble Metals

Junmei Wei and Enrique Iglesia*

Department of Chemical Engineering, University of California at Berkeley, Berkeley, California 94720

Received: October 5, 2003; In Final Form: January 21, 2004

Isotopic tracer and kinetic studies are used to probe the identity and reversibility of elementary steps required for H_2O and CO_2 reforming of CH_4 on supported Pt clusters and to demonstrate a rigorous kinetic and mechanistic equivalence for CO_2 and H_2O reforming, CH_4 decomposition, and water-gas shift reactions. Reforming rates are exclusively limited by C−H bond activation on essentially uncovered Pt crystallite surfaces and unaffected by the concentration or reactivity of co-reactants (H_2O, CO_2). Kinetic isotopic effects are consistent with the sole kinetic relevance of C−H bond activation ($k_H/k_D = 1.58-1.77$ at 873 K); these isotope effects and measured activation energies are similar for H_2O reforming, CO_2 reforming, and CH_4 decomposition reactions. CH_4/CD_4 cross exchange rates are much smaller than the rate of methane chemical conversion in CO_2 and H_2O reforming reactions; thus, C−H bond activation steps are irreversible, except as required by the approach to equilibrium for the overall reforming reaction. Reactions of $^{12}CH_4/^{12}CO_2/^{13}CO$ mixtures led to identical ^{13}C fractions in CO and CO_2, indicating that CO_2 activation is quasi-equilibrated and kinetically irrelevant. Binomial water and dihydrogen isotopomer distributions during reactions of $CH_4/CO_2/D_2$ mixtures indicate that these products form in quasi-equilibrated steps. Turnover rates for H_2O and CO_2 reforming and CH_4 decomposition increased with increasing Pt dispersion, suggesting that coordinative unsaturated surface Pt atoms, prevalent in small crystallites, are more reactive than Pt atoms in low-index surfaces for C−H bond activation. Pt dispersion but not turnover rates were influenced by the identity of the support (ZrO_2, γ-Al_2O_3, ZrO_2-CeO_2). Similar CO oxidation rates were measured before and after CH_4 reactions, indicating that Pt dispersion is not affected by unreactive deposits or sintering during catalysis. These mechanistic conclusions and metal dispersion effects appear to apply generally to CH_4 reactions on Group VIII metals, but the surface reactivity of Pt clusters in C−H bond activation reactions is greater than for similar size clusters of other metals. Turnover rates are compared here, for the first time, for most catalytically important noble metals (Rh, Ir, Pt, Ru) as a function of their metal dispersion on several supports. These turnover rates rigorously exclude transport and thermodynamic artifacts and provide a direct comparison of the reactivity of noble metal clusters for catalytic reactions of CH_4 on materials and at conditions relevant to industrial practice.

1. Introduction

CH_4 reactions with CO_2 or H_2O on supported Ni,[1,2] Rh,[3,4] Ru,[5,6] Ir,[7] and Pt[2,3,8−32] lead to H_2/CO mixtures useful as precursors to fuels and petrochemicals. Pt appears to be one of the most active and stable metals for these reactions.[13,19−23] Pt/ZrO_2, for instance, has been used in CH_4-CO_2 reactions for 500 h without detectable deactivation.[21−23] Rigorous comparisons among different metals are difficult because of ubiquitous transport and thermodynamic artifacts and of incomplete assessments of the number and cleanliness of exposed metal atoms.

Redox cycles involving parallel CH_4 activation on Pt clusters and CO_2 dissociation on reduced support sites were proposed for CH_4-CO_2 reactions on Pt/ZrO_2.[11] Such cycles would turn over with rates dependent on the relative abundance and reactivity of metal and support sites, which must act in concert to activate CH_4 and remove carbon atoms via reactions with CO_2 (or H_2O). Infrared spectra of CO_2 adsorbed on Pt/Al_2O_3, Pt/TiO_2, and Pt/ZrO_2 at 775 K indicated that carbonates formed on supports, which led to the proposal that Pt activates CH_4 and chemisorbed carbon reacts with carbonates at metal−support interfaces.[19−22] CO_2-CH_4 reforming at interfaces on Ni catalysts[33] were later proposed also for Pt-based catalysts.[9,10] This proposal claimed that CH_4 activation reversibly formed adsorbed CH_x and H species on Pt and then reacted with CO_2 dissociation fragments in equilibrated steps that form CH_xO, which irreversibly decomposed to CO and H_2 and led to a complex rate equation:

$$r_{CH_4} = \frac{aP_{CH_4}P_{CO_2}}{bP_{CO}P_{H_2}^{(4-x)/2} + (1 + cP_{CH_4})P_{CO_2}} \quad (1)$$

where x is the number of H-atoms in CH_xO.

Rostrup-Nielsen and Hansen[2] reported similar activation energies for CO_2 and H_2O reforming with CH_4 on Pt/MgO, suggesting that the two reactions share kinetically relevant steps. Yet, measured reforming rates were about five times greater with H_2O than with CO_2 co-reactants, a finding attributed to rate-determining CO_2 dissociation steps during CH_4-CO_2 reactions, despite the similar measured activation energies.

The effects of surface structure on reaction rates remain unresolved for CH_4 reactions on metal catalysts. Several studies showed that C−H bond activation in alkanes is structure-

* Author to whom correspondence should be addressed. Tel: (510)-642-9673. Fax: (510)-642-4778. E-mail: iglesia@cchem.berkeley.edu.

10.1021/jp036985z CCC: $27.50
Published on Web 03/10/2004

TABLE 1: Pt Dispersion (*D*), Crystallite Diameter (*d*), and Forward CH_4 Turnover Rates on Pt-Based Catalysts (873 K, 20 kPa CH_4, 25 kPa CO_2 or H_2O, 100 kPa Total Pressure, Balance Ar)

			forward CH_4 turnover rate (s^{-1})		
catalyst	Pt dispersion	crystallite diameter (nm)[b]	CH_4-CO_2	CH_4-H_2O	CH_4 decomposition[c]
1.6 wt % Pt/ZrO_2-CeO_2[a]	0.256	3.9	15.0	14.8	
0.8 wt % Pt/ZrO_2-CeO_2	0.345	2.9	18.6	19.5	
0.4 wt % Pt/ZrO_2-CeO_2	0.435	2.3	21.1	22.5	18.6
0.2 wt % Pt/ZrO_2-CeO_2	0.572	1.7	23.8	24.7	
1.6 wt % Pt/ZrO_2	0.159	6.3	12.8	13.1	12.4
0.8 wt % Pt/ZrO_2	0.276	3.6	16.4	16.9	15.8
0.4 wt % Pt/ZrO_2	0.383	2.6		19.2	
1.6 wt % Pt/Al_2O_3	0.219	4.4	11.2	14.7	

[a] Zr/Ce(mole) = 4. [b] Estimated from fraction Pt dispersion using equation $D = 1/d$.[48] [c] Initial CH_4 decomposition turnover rate on Pt surface.

sensitive[4,34,35] by the definition of Boudart,[36] a conclusion consistent with experimental and theoretical studies on well-defined surfaces;[37−45] these latter studies indicate that coordinatively unsaturated surface atoms lead to higher CH_4 sticking and dissociation rates than atoms on close-packed surfaces. For instance, CH_4 dissociation rates using molecular beams are higher on Pt(533) at 600 K than on close-packed Pt(111) surfaces at even higher temperatures (800 K),[44] and alkane dissociation did not occur, except possibly at minority defect sites, on Pt(111).[45] CO_2-CH_4 and H_2O-CH_4 catalytic turnover rates increased with increasing Rh[3,4] and Ru[6] dispersion, consistent with higher rates on coordinatively unsaturated atoms. We have not found similar systematic studies of Pt dispersion effects on CH_4 reforming turnover rates.

Oxides used to support Pt clusters and metal−support interfaces are often implicated in bifunctional CH_4 reforming pathways, but they also determine metal dispersion and transport properties, and in doing so, can introduce thermodynamic and transport corruptions into kinetic measurements. CH_4 conversions during CH_4-CO_2 reactions were higher on Pt/ZrO_2 than on Pt/SiO_2 or Pt/Al_2O_3, a finding attributed to CO_2 dissociation on ZrO_2, but neither Pt dispersion nor turnover rates were measured.[11,12] Support effects would be detected when bifunctional pathways require Pt-support interfaces,[22] but they cannot influence reaction rates directly when C−H bond activation on metal surfaces is the only kinetically relevant step, as inferred from relative bond energies in CH_4 and CO_2 (or H_2O) and from studies on well-defined metal surfaces.

Detailed kinetic and isotopic studies of CH_4-H_2O, CH_4-CO_2, and CH_4 decomposition reactions on Pt are unavailable; reported reaction rates have not been, for the most part, corrected for approach to equilibrium, measured under kinetic-controlled conditions, or normalized by the number of exposed Pt atoms. We report here, for the first time, a comparison of CH_4 reaction turnover rates on catalytically relevant noble metals (Pt, Ir, Rh, Ru) for a wide range of metal dispersion (0.15−0.70) and supports. We also report kinetic and isotopic evidence for the identity and reversibility of elementary steps required for H_2O and CO_2 reforming of CH_4 on supported Pt clusters and demonstrate a rigorous kinetic and mechanistic equivalence for CO_2 and H_2O reforming, CH_4 decomposition, and water-gas shift reactions. These studies provide conclusive kinetic and isotopic evidence for the sole kinetic relevance of C−H bond activation and for the essentially uncovered state of Pt clusters during steady-state catalysis and for the general relevance of these conclusions to other noble metals. We also find that Pt surfaces are the most active metal among Group VIII metals for C−H bond activation and for CH_4 reforming with H_2O or CO_2. Turnover rates increased with increasing Pt dispersion on Al_2O_3, ZrO_2, and ZrO_2-CeO_2, but they did not depend on the identity of the support, as also found for Rh, Ir, and Ru catalysts. The activation of the co-reactant (CO_2 or H_2O) is fast relative to C−H bond activation steps and therefore not kinetically relevant. These conclusions are consistent with those recently reported for Rh[4] and Ru[6] clusters; they appear to apply generally to chemical conversion of CH_4 on Group VIII metals.

2. Experimental Methods

2.1. Synthesis and Characterization. Pt/Al_2O_3, Pt/ZrO_2, and Pt/ZrO_2-CeO_2 with varying Pt content (0.2−1.6 wt %) were prepared by incipient wetness impregnation of Al_2O_3, ZrO_2 and ZrO_2-CeO_2 with aqueous $H_2PtCl_6 \cdot 6H_2O$ solutions (Aldrich, Lot# 10013LO, 99%). Samples were dried in ambient air at 393 K and then treated in flowing dry air (Airgas, UHP, 1.2 $cm^3/g-s$) at 873 K (0.167 K s^{-1}) for 5 h. Samples were reduced in H_2 (Airgas, UHP, 50 $cm^3/g-s$) at 873 K (0.167 K s^{-1}) for 2 h. Al_2O_3 (160 m^2/g) was prepared by heating $Al(OH)_3$ (Aldrich, 21645−51−2) in flowing dry air (Airgas, UHP, 1.2 $cm^3/g-s$) at 923 K (0.167 K s^{-1}) for 5 h to form γ-Al_2O_3.[46] ZrO_2 (45 m^2/g) was prepared as previously described.[4] ZrO_2-CeO_2 (Zr/Ce = 4) was synthesized by hydrolysis of 0.5 M $ZrOCl_2 \cdot 8H_2O$ (Aldrich, >98 wt %) and $Ce(NO_3)_3$ (Alfa, CAS # 15336−18−2, 99.5%) at a constant *pH* of 10, maintained by controlled addition of 14.8 M NH_4OH. The precipitate was filtered and washed by re-dispersing powders in a NH_4OH solution (*pH* 10, ~333 K) until Cl ions were no longer detected by $AgNO_3$ (Cl^- < 10 ppm). ZrO_2-CeO_2 powders were then dried in ambient air at 393 K overnight and treated in flowing dry air (Airgas, UHP, 1.2 $cm^3/g-s$) at 923 K (0.167 K s^{-1}) for 5 h. Supported Rh, Ru, and Ir catalysts were also prepared by incipient wetness and detailed synthesis and characterization procedures are reported elsewhere.[4,6,47]

Pt dispersion was measured using volumetric methods from uptakes of strongly chemisorbed hydrogen at 373 K.[4,6] These dispersions (shown in Table 1) were used to estimate average crystallite diameters by assuming hemispherical geometry using:

$$D = 1/d \tag{2}$$

where *D* is the fractional dispersion and *d* is the crystallite diameter (in nm).[48]

2.2. Catalytic and Stoichiometric Reactions of Methane. The microreactor system was described previously (quartz or steel tube with 8 mm inner diameter and with a type K thermocouple enclosed within a sheath in contact with the catalyst bed).[4,6] Reaction rates were measured on catalysts (5 mg; 250−425 μm particles) diluted with inert support within the pellets (25 mg) and then diluted the catalyst bed with acid-

washed quartz powder (500 mg) of similar size. Reactant mixtures consisted of 50% CH_4/Ar (Matheson) and 50% CO_2/Ar (Matheson) certified mixtures with He (Airgas, UHP) as a diluent. H_2O was introduced using a syringe pump (Cole-Parmer, 74900 series), and transfer lines were kept above 373 K after H_2O introduction to avoid condensation. The effects of CH_4 and CO_2 pressures on CH_4 reaction rates were measured at 823−1023 K and 100−1000 kPa total pressure over a wide range of reactant concentrations. The effect of H_2O pressure on CH_4 reaction rates was measured at 823−1023 K and 100 kPa total pressure. Reactant and product concentrations were measured with a Hewlett-Packard model 6890 gas chromatograph equipped with a Carboxen 1000 packed column (3.2 mm × 2 m) and a thermal conductivity detector.

Pt/ZrO_2 (0.8, 1.6 wt %, 20 mg) and Pt/ZrO_2-CeO_2 (0.4 wt %, 20 mg) samples diluted with 500 mg of quartz powder were used to measure rates of CH_4 and CD_4 decomposition (without co-reactants) at 873−973 K. CH_4 conversions were measured by on-line mass spectrometry (Leybold Inficon, Transpector Series). Reactant mixtures with 20% CH_4/Ar or 20% CD_4/Ar were prepared using 50% CH_4/Ar (Matheson, certified mixture) or pure CD_4 (Isotec, chemical purity > 99.0%) and Ar (Airgas, UHP). Intensities at 15 and 18 amu were used to measure CH_4 and CD_4 effluent concentrations, respectively. Ar was used as an internal standard. Initial CH_4 decomposition rates were used to estimate rate constants for CH_4 decomposition, based on the observed linear dependence of decomposition rates on CH_4 partial pressures.

2.3. Isotopic Tracer Studies and Kinetic Isotope Effects. Isotopic tracer studies of CH_4 reforming reactions were carried out on 0.4 wt % Pt/ZrO_2-CeO_2 using a transient flow apparatus with short hydrodynamic delays (<5 s). Chemical and isotopic compositions were measured using on-line mass spectrometry (Leybold Inficon, Transpector Series). CD_4, D_2O (Isotec, chemical purity > 99.0%), 5% D_2/Ar, and ^{13}CO (Isotec, chemical purity > 99.0%) were used as reactants without further purification. Intensities at 15 and 17−20 amu were used to measure the concentration of methane isotopomers. CH_4 and CD_4 fragmentation patterns were measured and those for CHD_3, CH_2D_2, and CH_3D were calculated using reported methods.[49] Intensities at 18, 19, and 20 amu were used to determine water isotopomers and those at 28, 29, 44, and 45 amu to measure ^{12}CO, ^{13}CO, $^{12}CO_2$, and $^{13}CO_2$ concentrations, respectively. Kinetic isotope effects were measured from the relative reaction rates with CH_4/CO_2 and CD_4/CO_2 reactants for CO_2 reforming and with CH_4/H_2O, CD_4/H_2O, and CD_4/D_2O reactants for steam reforming. Detailed experimental conditions are shown with the corresponding data in the results section.

2.4. CO Oxidation Rates. CO oxidation was used as a structure-insensitive reaction to detect any changes in the number of exposed Pt atoms as a result of catalytic CH_4 reforming reactions. Pt/ZrO_2 (0.4, 0.8, and 1.6 wt %, 10 mg) catalysts diluted with 500 mg of quartz powder were used to measure CO oxidation reaction rates at 413 K, 0.19 kPa CO, and 0.19 kPa O_2. These rates were measured before and after reforming reactions by measuring reactant and product concentrations using gas chromatography and the same protocols described above for CH_4 reactions. Mixtures of 25% O_2/He (Matheson, certified mixture) and 81.5% CO/N_2 (Matheson, certified mixture) were used as reactants.

3. Results and Discussion

3.1. Kinetic Dependence of Forward CH_4 Reaction Rate on Partial Pressure of Reactants. The kinetic response of CH_4 reforming rates to CH_4, CO_2, and H_2O concentrations was measured on 1.6 wt % Pt/ZrO_2 at conditions leading to stable rates, without detectable carbon formation, sintering of metal particles, or transport artifacts. Figure 1 shows net CH_4 turnover rates as a function of residence time at 873 K on 1.6 wt % Pt/ZrO_2 with different pellet sizes and different diluent/catalyst ratios within pellets. Varying the diameter of catalyst pellets (250−425 vs 63−106 μm) or the extent of dilution within the pellets (5:1 to 10:1) did not influence CH_4 turnover rates (Figure 1), indicating that measured net rates are unaffected by transport artifacts. Undiluted pellets and beds, often used in previous studies, led to lower reaction rates as a result of mass and heat transfer restrictions. Forward CH_4 turnover rates were obtained from measured rates by rigorously correcting them for reactant depletion and approach to equilibrium in CO_2 (eq 3) or H_2O (eq 4) reforming reactions:

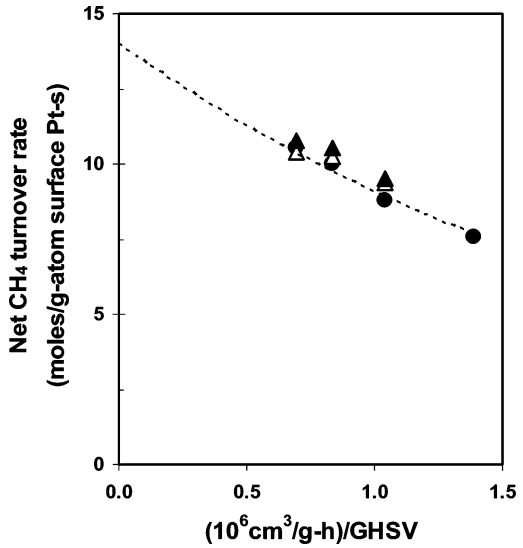

Figure 1. Net CH_4 turnover rates versus residence time for CH_4-CO_2 reaction on 1.6 wt % Pt/ZrO_2 (873 K, (●) 5 mg of catalyst diluted with 50 mg of Al_2O_3 within pellets, then diluted with 500 mg of ground quartz, pellet size 250−425 μm; (△) 5 mg of catalyst diluted with 25 mg of Al_2O_3 within pellets, then diluted with 500 mg of ground quartz, pellet size 250−425 μm; (▲) 5 mg of catalyst diluted with 25 mg of Al_2O_3 within pellets, then diluted with 500 mg of ground quartz, pellet size 63−106 μm).

$$\eta_1 = \frac{[P_{CO}]^2[P_{H_2}]^2}{[P_{CH_4}][P_{CO_2}]} \times \frac{1}{K_{EQ1}} \tag{3}$$

$$\eta_2 = \frac{[P_{CO}][P_{H_2}]^3}{[P_{CH_4}][P_{H_2O}]} \times \frac{1}{K_{EQ2}} \tag{4}$$

where $[P_j]$ is the average partial pressure of species j (in atm) within the catalyst bed and K_{EQ1} and K_{EQ2} are equilibrium constants[50] for each reaction at a given temperature. The fractional distance from equilibrium ($1 - \eta$) ranges from 0.70 to 0.97 for the experiments reported here. Net turnover rates (r_n) are used to obtain forward turnover rate (r_f) using

$$r_n = r_f(1 - \eta) \tag{5}$$

This equation accurately described all observed effects of reactor residence time on rates, as indicated by the curve in Figure 1. All rates reported from this point forward represent the rate of forward reforming reactions.

Figure 2 shows the effects of average CH_4, CO_2, and H_2O pressures, defined as the linear average of their inlet and outlet

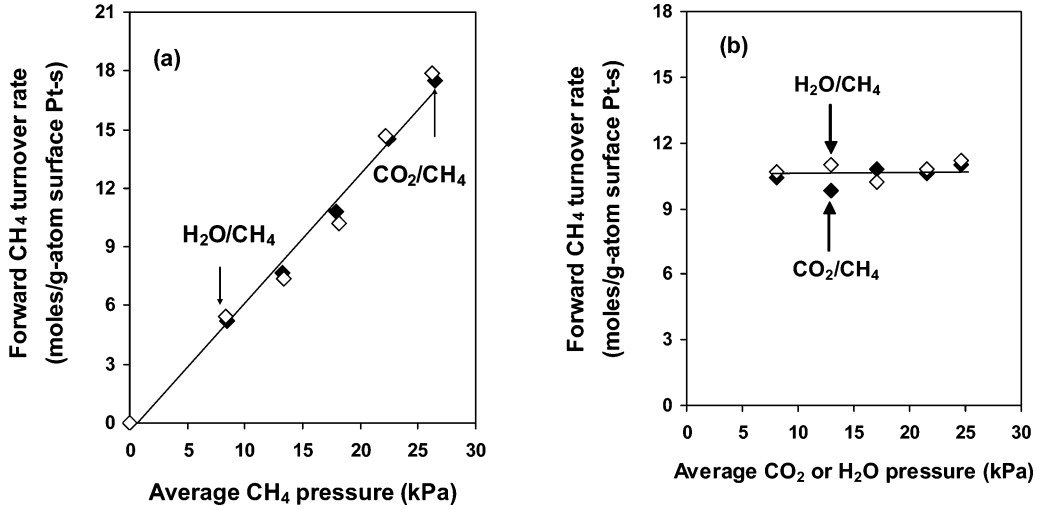

Figure 2. Effects of CH_4 (a) and CO_2 or H_2O (b) partial pressure on forward CH_4 turnover rate for CH_4-CO_2 and CH_4-H_2O reactions on 1.6 wt % Pt/ZrO_2 (5 mg of catalyst, 873 K, total flow rate 100 cm^3/min, 20 kPa CO_2 or H_2O in (a) and 20 kPa CH_4 in (b), balance He).

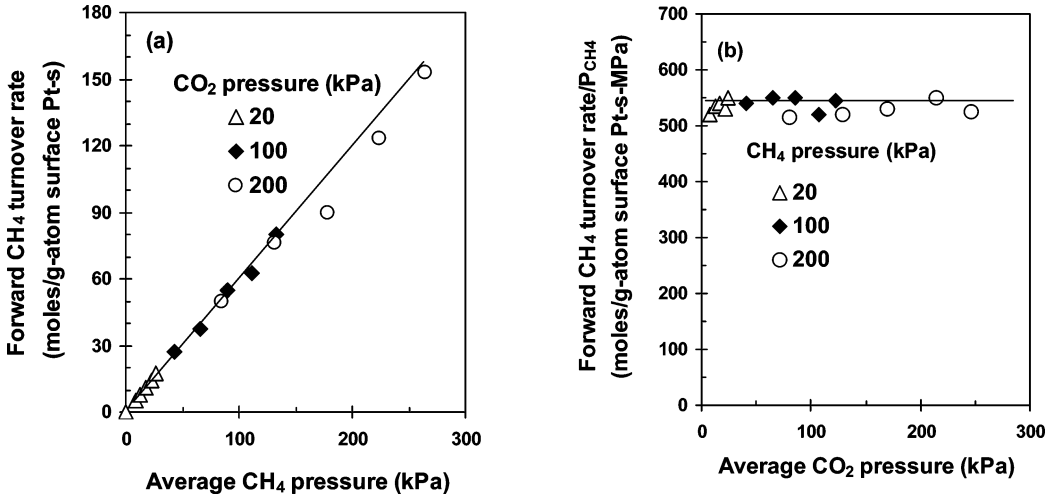

Figure 3. Effects of CH_4 (a) and CO_2 (b) average partial pressures on forward CH_4 turnover rate for CO_2 reforming of CH_4 on 1.6 wt % Pt/ZrO_2 (5 mg of catalyst, 873 K, total flow rate 100 cm^3/min, balance He, average pressure is the average of inlet and outlet pressures of the reactor).

values, on forward CH_4 turnover rates at 873 K on 1.6 wt % Pt/ZrO_2. This linear average is an accurate representation of the kinetic driving force for the small axial concentration gradients prevalent in this study, and becomes rigorous if reaction rates are first-order in CH_4, as shown by the data in Figure 2. Turnover rates for forward CO_2 and H_2O reforming reactions increased linearly with increasing CH_4 partial pressure (Figure 2a); they were not influenced by CO_2 or H_2O partial pressures (Figure 2b). Turnover rates were very similar for these two reactions, indicating that co-reactants are required by stoichiometry, but their activation or subsequent reactions are not kinetically relevant. Forward turnover rates were not influenced by CO and H_2 pressures (0−10 kPa), whether varied by changing residence time or by addition of H_2 or CO to CH_4-CO_2 or CH_4-H_2O reactants. These reaction products influence the approach to equilibrium (η) and thus net rates, but not forward rates (from eqs 3−5).

CH_4 reforming reactions can be accurately described by a first-order dependence on CH_4 and a zero-order dependence on CO_2, H_2O, H_2, or CO:

$$r_f = kP_{CH_4} \tag{6}$$

This first-order rate equation is identical for CH_4-CO_2 and CH_4-H_2O reactions at all reaction temperatures (823−1023 K) on all Pt-based catalysts examined here. Figure 3 shows the effects of CH_4 and CO_2 pressures on forward CH_4 turnover rates at 873 K over a much larger pressure range (100−1000 kPa). Forward CH_4 turnover rates increased linearly with increasing CH_4 partial pressure throughout this wider pressure range, which includes conditions relevant to industrial practice. Rates were not influenced by CO_2 pressure or by the pressure of H_2, CO, or H_2O formed during reaction.

Figure 2b shows that CH_4 turnover rates for H_2O and CO_2 reforming are similar for a given CH_4 pressure. These rates are also similar to those measured during the initial stages of CH_4 decomposition on 1.6 wt % Pt/ZrO_2 (without H_2O or CO_2 co-reactants) (Figure 4, Table 2). First-order rate constants for H_2O (k_{H_2O}) and CO_2 (k_{CO_2}) reforming and for CH_4 decomposition (k_{decomp}) are similar within experimental error at each temperature (Figure 5); this leads to activation energies for CO_2 (83 kJ mol^{-1}) and H_2O (75 kJ mol^{-1}) reforming and for CH_4 decomposition reactions (78 kJ mol^{-1}) that are also similar within our ability to measure them.

These similarities in turnover rates, rate constants, and activation energies for the three reactions indicate a common kinetically relevant step, which cannot involve species derived from co-reactants. The first-order CH_4 dependence and the measured kinetic insensitivity to co-reactants indicate that CH_4

TABLE 2: Forward CH_4 Reaction Rates, Rate Constants, Activation Energies, and Pre-exponential Factors for CH_4 Reactions on 1.6 wt % Pt/ZrO_2 (873 K, 20 kPa CH_4, 25 kPa CO_2 or H_2O, 100 kPa Total Pressure, Balance Ar)

co-reactant	turnover rate (s^{-1})[a]	rate constant (s^{-1} kPa^{-1})	activation energy (kJ/mol)	pre-exponential factor (s^{-1} kPa^{-1}) experimental	pre-exponential factor (s^{-1} kPa^{-1}) estimated[b]
CO_2	12.8	0.64	83	5.9×10^4	5.5×10^3
H_2O	13.1	0.66	75	2.0×10^4	5.5×10^3
None	12.4	0.62	78	2.9×10^4	5.5×10^3

[a] Initial CH_4 turnover rate on Pt surface. [b] Calculatedon the basis of transition-state theory treatments of CH_4 activation steps proceeding via an immobile activated complex.[51]

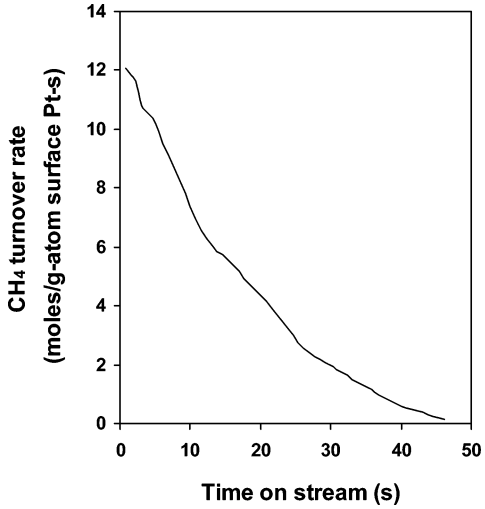

Figure 4. CH_4 decomposition rates on 1.6 wt % Pt/ZrO_2 as a function of time (873 K, 20 kPa CH_4, 100 kPa total pressure, balance Ar).

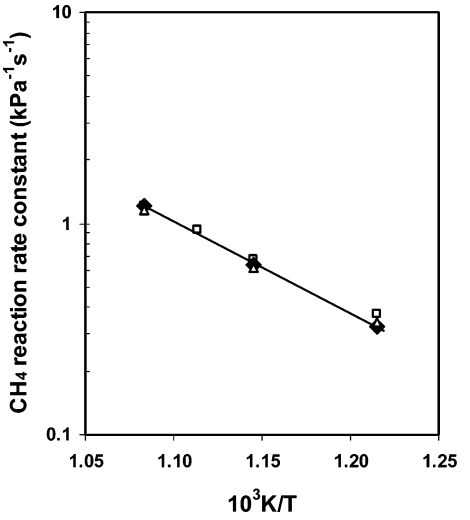

Figure 5. Arrhenius plots for CO_2 reforming (◆), H_2O reforming (□), and CH_4 decomposition (△) first-order rate constants on 1.6 wt % Pt/ZrO_2.

activation is the common kinetically relevant step. C−H bond activation on essentially uncovered Pt surfaces is the sole kinetically relevant step, and reactions of CO_2 or H_2O with CH_4-derived chemisorbed carbon species are fast, essentially quasi-equilibrated, and kinetically irrelevant.

If C−H bond activation is the sole kinetically relevant step in these three reactions, measured rate constants, preexponential factors can be estimated from transition state theory by merely assuming a degree of mobility for the relevant activated complex. Measured preexponential factors for these three reactions and those predicted by assuming immobile activated complexes[51] are compared in Table 2. Predicted preexponential factors are 3−10 times larger than experimental values, a level of agreement that is adequate in view of incompleteness of transition state treatments, and which can be improved by allowing modest two-dimensional mobility of activated complexes.

TABLE 3: Kinetic Isotope Effects for CH_4 Reactions on 1.6 wt % Pt/ZrO_2 (873 K, 25 kPa CH_4 or CD_4, 25 kPa CO_2, H_2O, or D_2O, 100 kPa total pressure, balance Ar)

	kinetic isotope effect		
	873 K	923 K	973 K
r_{CD_4/H_2O}:r_{CD_4/D_2O}	1.07	1.12	1.05
r_{CH_4/H_2O}:r_{CD_4/H_2O}	1.69	1.49	1.31
r_{CH_4/CO_2}:r_{CD_4/CO_2}	1.77	1.44	1.34
$r_{CH_4/none}$:$r_{CD_4/none}$	1.58		

3.2. Kinetic Isotope Effects. The kinetic relevance of C−H bond activation steps was confirmed by measuring isotope effects from forward turnover rates for CH_4-CO_2 and CD_4-CO_2 reactant mixtures at 873−973 K on 1.6 wt % Pt/ZrO_2. Kinetic isotope effects for H_2O reforming were similarly measured from forward turnover rates for CH_4-H_2O and CD_4-H_2O reactants. The irrelevance of co-reactant activation and of subsequent reactions of intermediates formed from water co-reactants were confirmed from the similar turnover rates measured with CD_4-H_2O and CD_4-D_2O mixtures. Kinetic isotope effects for CH_4 decomposition were measured from initial rates of CH_4 and CD_4 decomposition.

Normal kinetic isotopic effects were obtained for CH_4-CO_2 and CH_4-H_2O reactions and for CH_4 decomposition (Table 3); their values were identical within experimental accuracy for all three reactions at each reaction temperature. Kinetic isotope effect values at 873 K were 1.69, 1.77, and 1.58 for CO_2 reforming, H_2O reforming, and CH_4 decomposition, respectively. These results confirm the involvement of similar kinetically relevant C−H bond activation steps in these three reactions. CD_4-H_2O and CD_4-D_2O reactant mixtures gave similar turnover rates ($k_H/k_D = 1.05-1.12$), indicating that activation of co-reactants and any reactions involving adsorbed species formed from co-reactants are not involved in kinetically relevant steps.

Kinetic isotope effects for CH_4 activation on Pt(111)[34] and Pt(110)(1 × 2)[52,53] surfaces have been measured using molecular beam methods. Walker et al.[52] reported a kinetic isotope effect of 2 at 1000 K for CH_4 sticking probabilities on Pt(110) (1 × 2). We have not found previous kinetic isotope studies for catalytic H_2O and CO_2 reforming or for stoichiometric decomposition of CH_4 on Pt. The values reported here for Pt resemble those we have recently obtained in parallel studies on Ru (1.40−1.51),[6] Rh (1.54−1.60),[4] and Ni (1.62−1.71),[54] on which isotope effects were also similar for H_2O reforming, CO_2 reforming, and CH_4 decomposition; these values also resemble those reported by others for CH_4 decomposition on Ni (1.60) at 773 K.[55] Several studies,[56,57] however, detected no kinetic isotope effects for CO_2 reforming on Ni, apparently because near-

SCHEME 1: Sequence of Elementary Steps for CH_4 Reactions with H_2O or CO_2 on Pt Surfaces (⇒ irreversible step; ⇔ quasi-equilibrated step)

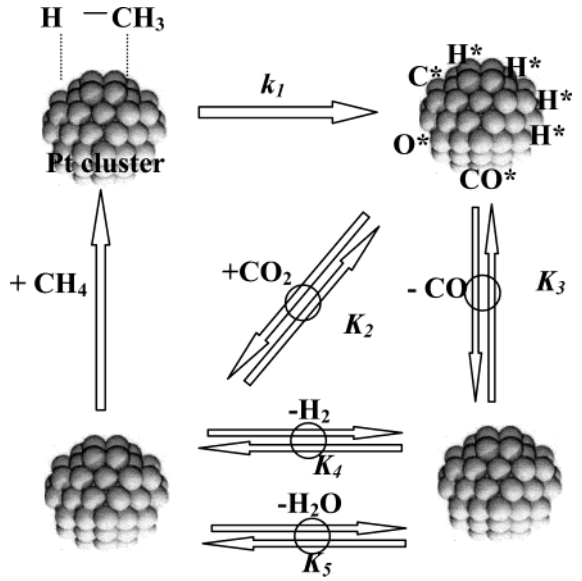

equilibrium methane conversions led to measurements of little kinetic relevance.

3.3. Elementary Steps in Chemical Conversion of Methane. The similar kinetic rate expressions for H_2O and CO_2 reforming and decomposition reactions, taken together with isotopic tracer studies and measured kinetic isotope effects, led us to propose a common sequence of elementary steps for CH_4 reactions on Ru,[6] Rh,[4] and Ni[54] catalysts. Here, we extend this mechanism, which contains all steps required for reforming, decomposition, and water-gas shift reactions, to Pt surfaces. Relevant elementary steps are shown in Scheme 1, where → denotes an irreversible step, and ⇔ represents a quasi-equilibrated step; k_i is the rate constant and K_i the equilibrium constant for step *i*.

CH_4 reacts in a sequence of elementary steps to form chemisorbed carbon and hydrogen. If unoccupied sites (*), corresponding to free Pt ensembles, are the most abundant reactive species, only the rate constant for step 1 (k_1) influences reaction rates; in this case, rates are proportional to CH_4 pressure and independent of the presence, identity, or specific concentration of CO_2 or H_2O co-reactants. CH_4 decomposition is followed by removal of CH_4-derived fragments using intermediates derived from CO_2 or H_2O co-reactants. Measured reactant and product concentrations during CH_4-CO_2 and CH_4-H_2O reactions indicate that water-gas-shift (WGS) reactions are equilibrated on Pt at all reaction conditions (Figure 6). Thus, elementary steps 2−5 in Scheme 1, which include all steps required for water-gas shift, must also be quasi-equilibrated during CH_4 reforming reactions.

Hickman and Schmidt[58] used a similar sequence and rate parameters reported on model surfaces to describe nonisothermal partial oxidation rates and selectivities on monolith-type Pt catalysts. O_2 dissociation and CO_2, CO, and H_2 formation and desorption were assumed to be reversible, while CH_4 dissociation was irreversible and assumed to have a activation energy of 43 kJ/mol, as reported on Pt(111).[59] The CO adsorption enthalpy of 128 kJ/mol used in their model,[58] would lead to CO coverages below 0.1% at 873 K, even at equilibrium CH_4 conversions; thus, no chemisorbed CO is expected during CH_4 reforming or partial oxidation on Pt-based catalysts at typical

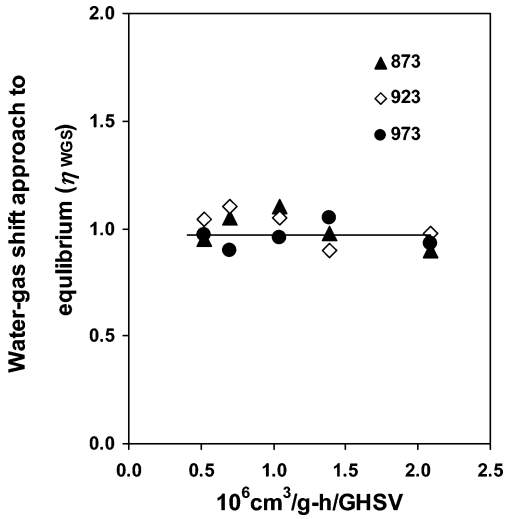

Figure 6. Water-gas-shift approach to equilibrium as a function of space velocity at 873 K on 1.6 wt % Pt/ZrO_2 (Reaction conditions: 25 kPa CO_2, 25 kPa CH_4, 100 kPa total pressure, balance Ar, $\eta_{WGS} = ([P_{CO}][P_{H_2O}])/([P_{H_2}][P_{CO_2}]K_{WGS})$).

reaction temperatures (800−1200 K), as we conclude also from the lack of kinetic inhibition by CO added to reactant streams.

3.4. Isotopic Tracer Studies of C−H Bond Activation Steps. The reversibility of C−H bond activation during CO_2 and H_2O reforming on Pt catalysts was probed by measuring rates of formation of deuterated isotopomers during reactions of $CH_4/CD_4/CO_2$ and $CH_4/CD_4/H_2O$ mixtures on 0.4 wt % Pt/ZrO_2-CeO_2 at 873−973 K. Reversible C−H bond activation would lead to similar chemical conversion and cross-exchange rates, because the latter merely reflects the reverse of C−H dissociation. Cross-exchange would occur more slowly than chemical conversion when C−H bond activation is irreversible.

Chemical conversion and isotopic scrambling rates were measured with $CH_4/CD_4/CO_2$ (1:1:2) or $CH_4/CD_4/H_2O$ (1:1:2) mixtures using on-line mass spectrometry, after removing $H_xD_{2-x}O$ at 218 K (to avoid interference between its fragments and those for CH_xD_{4-x}). CH_xD_{4-x} ($0 \le x \le 4$) formation and chemical conversion rates are shown in Figure 7 at 873 K. The CH_4/CD_4 cross exchange turnover rate, defined as the sum of CHD_3, CH_3D, and CH_2D_2 (twice) formation rates, is 1.9 s^{-1}, while the forward turnover rate for methane chemical conversion is 19.0 s^{-1}. The approach to equilibrium, η, during reaction was 0.10, while the ratio of the reverse (cross-exchange) to the forward (chemical conversion) CH_4 activation rates is also 0.10. This indicates that CHD_3, CH_2D_2, and CH_3D isotopomers form merely because the overall reaction itself approaches equilibrium and becomes reversible, which requires that the rate-determining step, when one exists, be exactly as reversible as the overall catalytic sequence. In effect, C−H bond activation on Pt at 873 K is irreversible, except for the extent to which reversibility is thermodynamically required by the approach to equilibrium for the overall chemical reaction.

CH_4/CD_4 cross exchange and chemical conversion rates are shown in Table 4 during reactions of $CH_4/CD_4/H_2O$ mixtures at several reaction temperatures. At all temperatures, methane chemical conversion rates are much higher than CH_4/CD_4 cross exchange rates; thus, kinetically relevant C−H bond activation steps are irreversible also during H_2O reforming reaction, except as required by overall thermodynamics.

3.5. Isotopic Tracer Studies of Co-Reactant Activation Steps. The reversibility of CO_2 activation steps (step 2 in Scheme 1) was determined from reactions of $^{12}CH_4/^{12}CO_2/^{13}CO$

TABLE 4: Methane Chemical Conversion and CH_4/CD_4 Cross Exchange Rates during Reaction of $CH_4/CD_4/H_2O$ Mixture on 0.4 wt % Pt/ZrO_2-CeO_2 Catalyst (12.5 kPa CH_4, 12.5 kPa CD_4, 25 kPa H_2O, 100 kPa total pressure, balance Ar)

reaction temperature(K)	methane chemical conversion turnover rate (s^{-1})[a]	cross exchange rate (s^{-1})[b]	$r_{exch}/r_{reaction}$[c]	η[d]
873	20.2	1.8	0.09	0.10
923	44.1	4.8	0.11	0.09
973	72.7	6.7	0.09	0.12

[a] Forward methane chemical conversion rate. [b] Total methane isotopomers formation rate. [c] Ratio of total methane isotopomers formation rate to the methane chemical conversion rate. [d] $\eta = ([P_{CO}][P_{H_2}]^3)/([P_{H_2O}][P_{CH_4}]\ K)$; approach to equilibrium for H_2O reforming reaction.

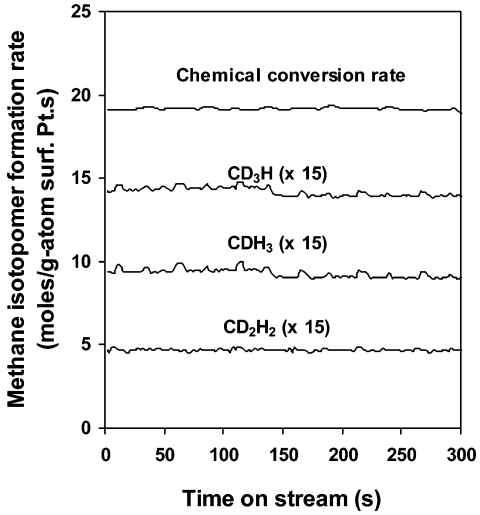

Figure 7. Methane turnover rates and CH_4/CD_4 cross exchange rates during the reaction of $CH_4/CD_4/CO_2$ mixture on 0.4% Pt/ZrO_2-CeO_2 catalyst (5 mg of catalyst, 873 K, 12.5 kPa CH_4 and CD_4, 25 kPa CO_2, 100 kPa total pressure, balance Ar).

reactants. Reversible CO_2 dissociation would lead to rapid formation of $^{13}CO_2$ via its microscopic reverse, while an irreversible step would preserve the isotopic purity of the $^{12}CO_2$ reactants.

Reactions of $^{12}CH_4/^{12}CO_2/^{13}CO$ (1:1:0.4) mixtures on 0.4 wt % Pt/ZrO_2-CeO_2 at 923 K led to similar ^{13}C fractions in the CO (0.25) and CO_2 (0.23) present in the reactor effluent, even though reactants were isotopically pure $^{12}CO_2$ and ^{13}CO. This ^{13}C content corresponds to complete chemical and isotopic equilibration between CO and CO_2, even at the low CH_4 conversion (15%) and approach to equilibrium ($\eta = 0.12$) prevalent in these experiments. These data confirm that CO_2 activation steps are much faster than the kinetically relevant steps for CH_4 chemical conversion to synthesis gas; thus, CO_2 activation steps must be quasi-equilibrated and kinetically irrelevant. In effect, steps 2 in Scheme 1 occur many times in both directions in the time scale required for a CH_4 chemical conversion turnover, a situation that also preserved surfaces essentially uncovered by CH_4-derived reactive intermediates. By inference from kinetic analogies between CH_4-CO_2 and CH_4-H_2O reactions, we conclude that H_2O activation steps are also likely to be quasi-equilibrated during H_2O reforming.

3.6. Isotopic Probes of Hydrogen and Hydroxyl Recombination Steps. Water forms during CO_2 reforming of CH_4 via reverse water-gas shift (RWGS) reactions. More rigorously, H_2O forms because chemisorbed O-atoms from CO_2 and chemisorbed H-atoms from CH_4 occasionally react to form water, in a reaction that is nonrigorously treated as a separate stoichiometric (water-gas shift) reaction in most previous studies. The expected reactants and products of water-gas shift reactions exist at their equilibrium relative concentrations during CH_4 reforming

TABLE 5: Distribution of Water Isotopomers during Reaction of $CH_4/CO_2/D_2$ Mixtures on 0.4 wt % Pt/ZrO_2-CeO_2 (873 K, 16.7 kPa CH_4, 16.7 kPa CO_2, 3.3 kPa D_2, 100 kPa Total Pressure, Balance Ar)

	distribution (%)	
isotopomer	measured (H/D = 1.43)	binomial (H/D[a] = 1.41)
H_2O	0.33	0.34
HDO	0.48	0.49
D_2O	0.16	0.17

[a] (H/D) ratio predicted from H in reacted methane and D_2 in ambient stream if complete mixing between the two isotopes occurred during reaction.

(Figure 6); thus, water and dihydrogen formation must involve quasi-equilibrated elementary steps.

The isotopic composition of products formed from $CH_4/CO_2/D_2$ (1:1:0.2) mixtures on 0.4 wt % Pt/ZrO_2-CeO_2 at 873−973 K was measured by on-line mass spectrometry. The H/D fraction expected if H-atoms in any CH_4 molecules converted to synthesis gas and D-atoms in the added D_2 contributed to surface intermediates is 1.41. The measured H/D ratios were 1.43 and 1.44 in water and dihydrogen, respectively, indicating complete equilibration between gas-phase dihydrogen and water molecules and their corresponding chemisorbed precursors. Water isotopomers formed from $CH_4/CO_2/D_2$ mixtures obey a binomial distribution (Table 5), as expected from quasi-equilibrated H* and OH* recombination (step 5 in Scheme 1). The quasi-equilibrated nature of the steps leading to water and dihydrogen, taken together with the expected equilibration of nondissociative CO chemisorption, would lead to thermodynamic equilibrium for water-gas shift reactions, as found experimentally. Binomial distributions were also observed for dihydrogen isotopomers at 873−973 K, as expected from reversible and quasi-equilibrated hydrogen recombinative desorption steps (step 4 in Scheme 1) during CH_4 reforming reactions.

3.7. Effects of Pt Dispersion and of Support on CH_4 Reactions. Methane activation studies on model surfaces have concluded that activation of C−H bonds depends sensitively on surface structure; specifically, surface steps and kinks are much more active than atoms on close-packed surfaces.[60−62] Surface roughness and coordinative unsaturation increase as metal clusters become smaller. To our knowledge, no systematic studies of Pt cluster size effects on CH_4 activation or reforming rates are available.

The effects of Pt dispersion on CH_4 reforming turnover rates are shown in Table 1 and Figure 8 for CH_4-CO_2, CH_4-H_2O, and CH_4 decomposition reactions. CH_4 turnover rates for each reaction increased monotonically with increasing Pt dispersion, suggesting that coordinatively unsaturated Pt surface atoms, prevalent in small crystallites, are indeed more active than atoms on the low-index surfaces predominately exposed on larger crystallites. Surface atoms with fewer Pt neighbors appear to bind CH_x and H species more strongly and to stabilize activated

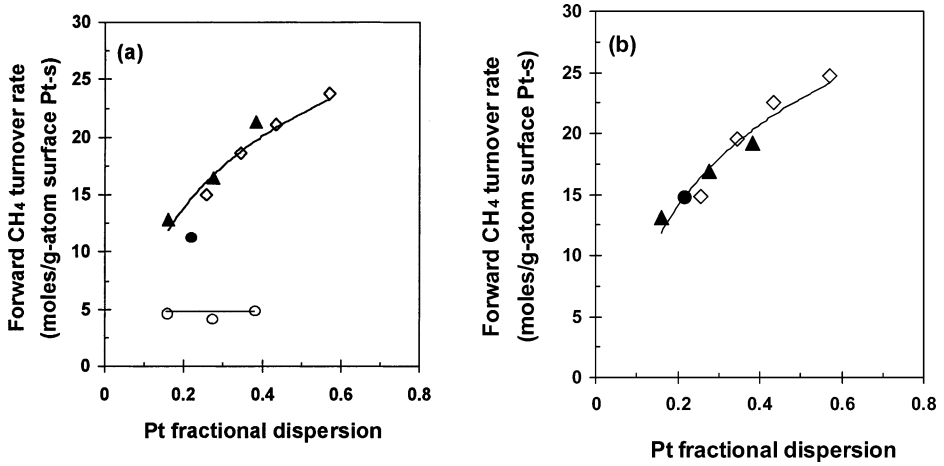

Figure 8. Forward CH_4 turnover rates for CO_2 (a) and H_2O (b) reforming of CH_4 as a function of Pt dispersion on various supports (873 K, 20 kPa CH_4, (▲) Pt/ZrO_2, (●) $Pt/\gamma\text{-}Al_2O_3$, (◇) Pt/ZrO_2-CeO_2, (○) CO turnover rate for CO oxidation at 413 K on Pt/ZrO_2).

complexes involved in the formation of these intermediates, thus decreasing C−H bond activation energies.

Thermal desorption and low-energy electron diffraction studies showed that the activation energy for dissociative chemisorption of ethane on Pt(110)−(1 × 2) surface is 25 kJ/mol lower than on close-packed Pt(111) surfaces.[63,64] Activation barriers for dissociation of CH_4 molecular beams on stepped Pt(533) surfaces were 30 kJ/mol lower than that on close-packed Pt(111).[43] *n*-Butane and *n*-pentane adsorbed dissociatively on Pt(110)−(1 × 2) but not on Pt(111) at 250 K.[65] Alkane reactions were not detected on Pt(111) in one ultrahigh vacuum study.[39] Molecular beam methods showed that initial ethane trapping probabilities on open Pt(110)−(1 × 2) surfaces were greater than on close-packed Pt(111).[66] These effects of coordinative unsaturation appear to be ubiquitous for molecule dissociation reactions. In fact, theory and experiment showed that N_2 dissociation on Ru is about 10^9 times faster on steps than on terraces;[67] activation barriers on steps were about 150 kJ/mol smaller than on terraces. Molecular beam studies showed that H_2 dissociation is nonactivated on stepped Pt(332), but proceeds with an activation barrier of 2−6 kJ/mol on Pt(111).[68]

Figure 8 and Table 1 also show the effects of support on forward CH_4 turnover rates for CH_4 reforming and decomposition reactions on Pt-based catalysts. The identity of the support did not influence measured turnover rates, but it can influence Pt dispersion. Once measured rates are rigorously normalized by the number of exposed Pt surface atoms, CH_4 reaction rates depend only on the size (and structure) of Pt clusters and not on the identity of the support. In any case, any potential involvement of the support in activation of CO_2 and H_2O co-reactants is inconsequential, because reaction rates depend only on C−H bond activation rates.

One study[11] reported much higher conversions during CO_2 reforming on Pt/ZrO_2 than on Pt/SiO_2 and suggested that ZrO_2 promotes CO_2 dissociation, but neither Pt dispersions nor turnover rates were reported. Thus, these support effects may reflect secondary effects of supports on Pt dispersion or on the extent to which mass or heat transfer influenced reaction rates. Another study[22] suggested that CH_4 conversion is controlled by Pt-support contact perimeter, because of the bifunctional nature of CO_2-CH_4 reforming pathways on Pt. These support effects are inconsistent with the kinetic irrelevance of co-reactant activation, shown here for reaction conditions resembling those in these previous studies, or with the lack of support effects reported in this study.

Similar dispersion and supports effects and similar actual values of turnover rates were measured for CH_4-H_2O, CH_4-CO_2, CH_4 decomposition reactions on the Pt catalysts of this study (Table 1, Figure 8), as expected from the rigorous mechanistic equivalence among these reactions. Similar effects of metal dispersion, also equivalent for all three reactions, were measured in parallel studies of CH_4 reforming and decomposition reactions on Rh,[4] Ru,[6] and Ir[47] catalysts.

Figure 9 shows similar effects of metal dispersion on turnover rates for CH_4-CO_2 and CH_4-H_2O reactions on other supported noble metals (Rh, Ir, Ru) in addition to the Pt catalysts of this study. For each metal, at least two supports were used to disperse metal clusters and no effects of support on turnover rates were detected. On all metals, CH_4 turnover rates increase with increasing metal dispersion. Pt surfaces are more active than those of the other noble metals for any given cluster size. This appears to be the first rigorous and direct comparison of the reactivity of supported Group VIII metal clusters for catalytic reactions of CH_4 using materials and conditions relevant to industrial practice. The exclusion of transport artifacts and reverse reactions and the measurement of rates normalized by the relevant exposed surface area of metal clusters make these rate comparisons a rigorous and sole reflection of the kinetic reactivity of such metal surfaces.

3.8. Characterization of Supported Pt Clusters by CO Oxidation. Here, we confirm the accuracy of chemisorptive Pt dispersions measured before reaction and their relevance to the state of Pt surfaces in working catalysts. These measurements are critical to ensure that observed dispersion effects and measured activation energies do not reflect blockage of exposed Pt atoms by unreactive carbon residues during initial catalytic turnovers, which could occur to varying extents as metal dispersion or reaction conditions vary. We note that we have not detected any transient effects during the first few seconds of exposure to CH_4-CO_2 or CH_4-H_2O reactants, but typical turnover times are short (<0.1 s), and any such initial transients may not be detected when they occur concurrently with short but unavoidable hydrodynamic delays (∼2 s).

These measurements also address significant differences between activation energies obtained from sticking coefficients on model surfaces and from chemical conversion and stoichiometric decomposition rates of CH_4 on supported Pt catalysts, which may reflect changes in the state of catalytic surfaces during reaction. Activation energies reported here (83 and 75 kJ/mol for CO_2 and H_2O reforming, respectively) and in previous CO_2 reforming studies on Pt-based catalysts[3,9,10] (63−96 kJ/mol) are much larger than those measured or calculated on model Pt surfaces.[35,59,69] For example, atom-superposition

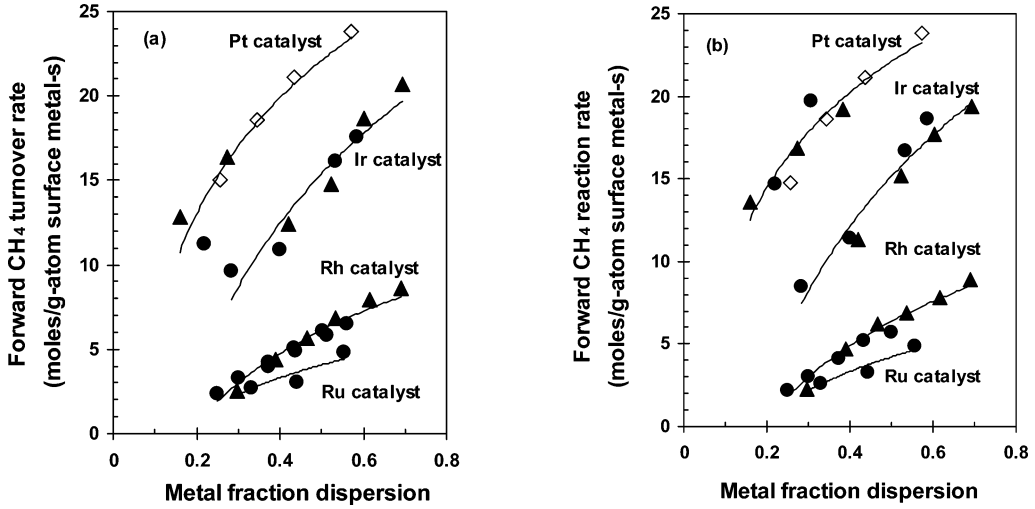

Figure 9. Forward CH_4 turnover rates for CO_2 (a) and H_2O (b) reforming of CH_4 as a function of metal dispersion on various supports (873 K, 20 kPa CH_4, (▲) ZrO_2, (●) γ-Al_2O_3, (◇) ZrO_2-CeO_2 as support).

electron-delocation molecular orbital methods gave an activation barrier of 43 kJ/mol for CH_4 activation on Pt(111) surfaces.[59] Activation energies of 20 and 35 kJ/mol were reported for the CH_4 sticking coefficient using molecular beam methods on Pt(110) (1 × 2) and Pt(111), respectively.[35,69]

Our kinetic study indicates that reactions of H_2O or CO_2 with CH_4-derived chemisorbed carbon are fast and lead to essentially uncovered surfaces during CH_4 reforming reactions. Yet, we cannot rule out that unreactive carbonaceous deposits, without detectable reactivity in reactions with co-reactants, form during the first few turnovers. For example, sites with the greatest coordinative unsaturation and reactivity could form irreversibly chemisorbed carbon, leaving less reactive surface Pt atoms to catalyze CH_4 conversion turnovers. These carbon deposits must be totally unreactive during CH_4 reforming, because their surface density would otherwise vary with the concentration or reactivity of the co-reactant, leading to apparent positive orders in the co-reactant reactant concentration and to different rates with H_2O and CO_2.

Here, we use CO oxidation, a recognized structure-insensitive reaction[70,71] (see also insensitivity of turnover rates to dispersion in Figure 8a) to detect any changes in the number of exposed Pt atoms during CH_4 reforming, whether these changes occur via blockage of surface sites or sintering of small Pt clusters. We note that chemisorption measurements after reaction are not possible, because of the very small catalyst amounts required for isothermal rate measurements (5 mg). CO oxidation rates on a fresh 1.6 wt % Pt/ZrO_2 catalyst and on this catalyst after CO_2 and H_2O reforming are identical within experimental accuracy (Figure 10). This shows unequivocally that the number of exposed Pt atoms is unchanged during reaction and that unreactive carbon residues are present at very low coverages (<5%), if at all.

We cannot rule out that some initially exposed surface atoms, with remarkable reactivity in stoichiometric CH_4 activation but unable to turn over, become unavailable during initial contact with reforming reactants and do not contribute to catalytic rates. Their number would have to be extremely small, because CO oxidation rates would otherwise be detectably influenced by CH_4 reforming reactions. We conclude, however, that such sites, if present, cannot turn over; thus, they are not relevant to the analysis and prediction of catalytic rates of CH_4-H_2O and CH_4-CO_2 reactions. These results raise important questions about the nature of model surfaces and methods that are

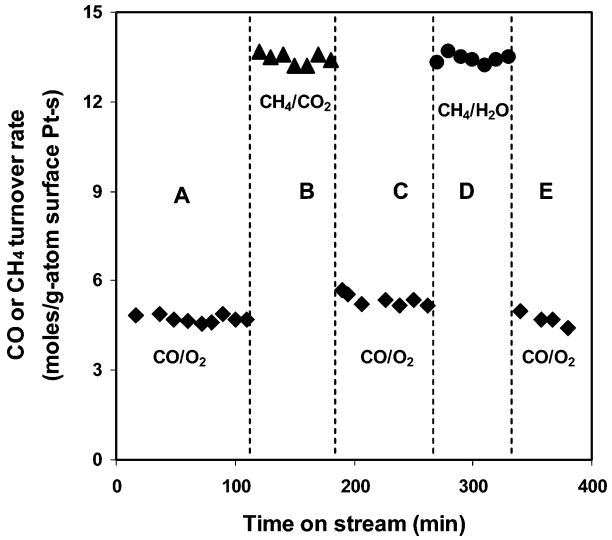

Figure 10. CO oxidation and forward CH_4 reforming turnover rates on 1.6 wt % Pt/ZrO_2 (A, C, E, CO oxidation turnover rates, 413 K, 0.19 kPa CO, 0.19 kPa O_2; B, CO_2 reforming turnover rates, 873 K, 25 kPa CH_4, 25 kPa CO_2; D, H_2O reforming turnover rates, 873 K, 25 kPa CH_4, 25 kPa H_2O).

appropriate for experimental and theoretical studies of CH_4 reactions. They also highlight the essential requirement that experiment and theory rigorously address complete catalytic cycles, and not merely stoichiometric steps presumably involved in such cycles.

4. Conclusions

Isotopic tracer and kinetic measurements led to a simple mechanistic picture and a unifying kinetic treatment of CH_4-CO_2, CH_4-H_2O, and CH_4 decomposition reactions, as well as water-gas shift, on Pt-based catalysts. Reforming and decomposition rates were first-order in CH_4 concentration and independent of the concentration or identity of the co-reactants, suggesting that reaction rates are exclusively limited by C−H bond activation on metal cluster surfaces and that co-reactant activation is not kinetically relevant. These conclusions are consistent with the similar activation energies measured for CH_4 reforming and decomposition reactions. The normal CH_4/CD_4 kinetic isotope effects measured were similar for all three CH_4 reactions and thus also independent of co-reactant identity.

Water and dihydrogen formation steps are quasi-equilibrated, as shown from their binomial isotopomers distributions during reactions of $CH_4/CO_2/D_2$ mixtures. The identical ^{13}C contents in CO and CO_2 molecules during $^{12}CH_4/^{12}CO_2/^{13}CO$ reactions indicate that CO_2 activation steps are reversible and quasi-equilibrated. The quasi-equilibrated nature of these steps in consistent with the observed chemical equilibrium among reactants and products of the water-gas shift.

Forward CH_4 turnover rates increased monotonically with increasing Pt dispersion for CO_2 reforming, H_2O reforming, and CH_4 decomposition reactions, suggesting that coordinative unsaturation increases C−H bond activation reactivity. Supports (ZrO_2, γ-Al_2O_3, ZrO_2-CeO_2) influence Pt dispersion, but not turnover rates, indicating that co-reactant activation on supports, if it occurs, is not kinetically relevant. The rates of structure-insensitive CO oxidation reactions are similar before and after CH_4 reforming; thus, the latter reaction does not influence the number of exposed Pt atoms via sintering or blockage by unreactive chemisorbed species.

These metal dispersion effects and the mechanistic conclusions reached from kinetic and isotopic studies are similar to those found in parallel studies of supported Rh, Ru, Ir, and Ni catalysts and appear to apply in general to CH_4 reactions on Group VIII metals. Pt surfaces, however, are the most reactive among the metal clusters examined.

Acknowledgment. This study was supported by BP as part of the Methane Conversion Cooperative Research Program at the University of California at Berkeley. Helpful technical discussions with Drs. John Collins and Theo Fleisch (BP) throughout these studies are gratefully acknowledged.

References and Notes

(1) Bradford, M. C. J.; Vannice, M. A. *Appl. Catal. A* **1996**, *142*, 97.
(2) Rostrup-Nielsen, J. R.; Bak Hansen, J. H. *J. Catal.* **1993**, *144*, 38.
(3) Zhang, Z. L.; Tsipouriari, V. A.; Efstathiou, A. M.; Verykios, X. E. *J. Catal*. **1996,** *158*, 51.
(4) Wei, J.; Iglesia, E. *J. Catal.*, in press.
(5) Bradford, M. C. J.; Vannice, M. A. *J. Catal.* **1999**, *183*, 69.
(6) Wei, J.; Iglesia, E. *J. Phys. Chem. B*, in press.
(7) Erdohelyi, A.; Fodor, K.; Solymosi, F. *Stud. Surf. Sci. Catal*. **1991**, *107*, 525.
(8) Ashcroft, A. T.; Cheetham, A. K.; Green, M. L. H.; Vernon, P. D. F. *Nature* **1991**, *352*, 225.
(9) Bradford, M. C. J.; Vannice, M. A. *J. Catal.* **1998**, *173*, 157.
(10) Bradford, M. C. J.; Vannice, M. A. *Catal. Lett.* **1997**, *48*, 31.
(11) Stagg, S. M.; Romeo, E.; Resasco, D. E. *J. Catal*. **1998**, *178*, 137.
(12) Noronha, F. B.; Fendley, E. C.; Soares, R. R.; Alvarez, W. E.; Resasco, D. E. *Chem. Eng. J.* **2001**, *82*, 21.
(13) Stagg, S. M.; Noronha, F. B.; Fendley, E. C.; Resasco, D. E. *J. Catal*. **2000**, *194*, 240.
(14) Souza, M. M. V. M.; Aranda, D. A. G.; Schmal, M. *J. Catal.* **2001**, *204*, 498.
(15) Souza, M. M. V. M.; Aranda, D. A. G.; Schmal, M. *Ind. Eng. Chem. Res.* **2002**, *41*, 4681.
(16) Chen, Y.; Liaw, B.; Lai, W. *Appl. Catal. A: General* **2002**, *230*, 73.
(17) Chen, Y.; Liaw, B.; Kao, C.; Kou, J. *Appl. Catal. A: General* **2001**, *217*, 23.
(18) Nagaoka, K.; Seshan, K.; Aika, K.; Lercher, J. A. *J. Catal.* **2001,** *197*, 34.
(19) Bitter, J. H.; Seshan, K.; Lercher, J. A. *Top. Catal*. **2000**, *10*, 295.
(20) Bitter, J. H.; Seshan, K.; Lercher, J. A. *J. Catal.* **1999**, *183*, 336.
(21) Bitter, J. H.; Seshan, K.; Lercher, J. A. *J. Catal.* **1997**, *171*, 279.
(22) Bitter, J. H.; Seshan, K.; Lercher, J. A. *J. Catal.* **1998**, *176*, 93.
(23) Lercher, J. A.; Bitter, J. H.; Hally, W.; Niessen, W.; Seshan, K. *Stud. Surf. Sci. Catal*. **1996**, *101*, 463.
(24) Nagaoka, K.; Seshan, K.; Lercher, J. A.; Aika, K. *Catal. Lett*. **2000**, *70*, 109.
(25) Mo, L.; Fei, J.; Huang, C.; Zheng, X. *J. Mol. Catal. A* **2003**, *193*, 177.
(26) Kim, G. J.; Cho, D. S.; Kim, K. H.; Kim, J. H. *Catal. Lett*. **1994**, *28*, 41.
(27) Qin, D.; Lapszewicz, J.; Jiang, X. *J. Catal.* **1996**, *159*, 140.
(28) Otsuka, K.; Ushiyama, T.; Yamanaka, I. *Chem. Lett.* **1993**, 1517.
(29) Solymosi, F.; Kustan, G.; Erohelyi, A. *Catal. Lett.* **1991**, *11*, 149.
(30) Sakai, Y.; Saito, H.; Sodesawa, T.; Nozaki, F. *React. Kinet. Catal. Lett*. **1984**, *24*, 253.
(31) Tokunaga, O.; Osada, Y.; Ogasawara, S. *Fuel* **1989**, *68*, 990.
(32) Mattos, L. V.; Rodino, E.; Resasco, D. E.; Passos, F. B.; Noronha, F. B. *Fuel Proc. Technol.* **2003**, *83*, 147.
(33) Bradford, M. C. J.; Vannice, M. A. *Appl. Catal. A* **1996**, *142*, 97.
(34) Luntz, A. C.; Bethune, D. S. *J. Chem. Phys.* **1989**, *90*, 1274.
(35) Reeves, C. T.; Seets, D. C.; Mullins, C. B. *J. Mol. Catal. A* **2001**, *167*, 207.
(36) Boudart, M. *Adv. Catal*. **1969**, *20*, 153.
(37) Weinberg, W. H. *Surv. Prog. Chem*. **1983**, *10*, 1.
(38) Szuromi, P. D.; Weinberg, W. H. *Surf. Sci.* **1984**, *145*, 407.
(39) Firment, L. E.; Somorjai, G. A. *J. Chem. Phys.* **1977**, *66*, 2901.
(40) Salmeron, M.; Somorjai, G. A. *J. Phys. Chem.* **1982**, *86*, 341.
(41) Choudhary, T. V.; Goodman, D. W. *J. Mol. Catal. A* **2000**, *163*, 8.
(42) Burghgraef, H.; Jansen, A. P.; van Santen, R. A. *Faraday Discuss*. **1993**, *96*, 337.
(43) Watwe, R. M.; Bengaard, H. S.; Rosrrup-Nielsen, J. R.; Dumesic, J. A.; Norskov, J. K. *J. Catal.* **2000**, *189*, 16.
(44) Gee, A. T.; Hayden, B. E.; Mormiche, C.; Kleyn, A. W.; Riedmuller, B. *J. Chem. Phys*. **2003**, *118*, 3334.
(45) Szuromi, P. D.; Engstrom, J. R.; Weinberg, W. H. *J. Phys. Chem.* **1985**, *89*, 2497.
(46) Bahlawane, N.; Watanabe, T. *J. Am. Ceram. Soc*. **2000**, *83*, 2324.
(47) Wei, J.; Iglesia, E. *Angew. Chem. Int. Ed.*, in press.
(48) Boudart, M.; Djega-Mariadassou, G. *The Kinetics of Heterogeneous Catalytic Reactions;* Princeton University Press: Princeton, NJ, 1984.
(49) Price, G. L.; Iglesia, E. *Ind. Eng. Chem*. **1989**, *28*, 839.
(50) Stull, D. R.; Edgar, F.; Westrum, J.; Sinke, G. C. In *The Thermodynamics of Organic Compounds*; Robert E. Krieger Publishing Co.: Malabar, FL, 1987.
(51) Dumesic, J. A.; Rudd, D. F.; Rekoske, J. E.; Trevino, A. A. *The Microkinetics of Heterogeneous Catalysis*; American Chemical Society: Washington, DC, 1993.
(52) Walker, A. V.; King, D. A. *J. Chem. Phys*. **2000**, *112*, 4739.
(53) Luntz, A. C.; Winter, W. H. *J. Chem. Phys.* **1994**, *101*, 10980.
(54) Wei, J.; Iglesia, E. *J. Catal.*, in press.
(55) Otsuka, K.; Kobayashi, S.; Takenaka, S. *J. Catal*. **2001**, *200*, 4.
(56) Schuurman, Y.; Kroll, V. C. H.; Ferreira-Aparicio, P.; Mirodatos, C. *Catal. Today* **1997**, *38*, 129.
(57) Kroll, V. C. H.; Swaan, H. M.; Lacombe, S.; Mirodatos, C. *J. Catal*. **1997**, *164*, 387.
(58) Hickman, D. A.; Schmidt, L. D. *AIChE J*. **1993**, *39*, 1164.
(59) Anderson, A. B.; Maloney, J. J. *J. Phys. Chem.* **1988**, *92*, 809.
(60) McMaster, M. C.; Madix, R. J. *J. Chem. Phys*. **1993**, *98*, 15.
(61) Liu, Z.; Hu, P. *J. Am. Chem. Soc.* **2003**, *125*, 1958.
(62) Klier, K.; Hess, J. S.; Herman, R. G. *J. Chem. Phys*. **1997**, *107*, 4033.
(63) Johnson, D. F.; Weinberg, H. *Science* **1993**, *261*, 5117.
(64) Johnson, D. F.; Weinberg, H. *J. Chem. Phys*. **1995**, *103*, 5833.
(65) Seuromi, P. D.; Engstrom, J. R.; Wittrig, T. S.; Weinberg, W. H. *J. Vac. Sci. Technol. A* **1985**, *3*, 1560.
(66) Stinnett, J. A.; McMaster, M. C.; Schroeder, S. L. M.; Madix, R. J. *Surf. Sci.* **1996**, *365*, 683.
(67) Dahl, S.; Logadottir, A.; Egeberg, R. C.; Larsen, R. C.; Chorkendorff, I. *Phys. Rev. Lett.* **1999**, *83*, 1814.
(68) Salmeron, M.; Gale, R. J.; Somorjai, G. A. *J. Chem. Phys*. **1979**, *70*, 2807.
(69) Arumainayagam, C. R.; Mcmaster, M. C.; Schoofs, G. R.; Madix, R. J. *Surf. Sci.* **1989**, *222*, 213.
(70) Boudart, M.; Rump, F. F. *React. Kinet. Catal. Lett.* **1987**, *135*, 95.
(71) Engel, G.; Ertl, G. *J. Chem. Phys*. **1978**, *69*, 1267.